Antiepileptic drugs and apoptotic neurodegeneration in the developing brain

Petra Bittigau*, Marco Sifringer*, Kerstin Genz*, Ellen Reith*, Dana Pospischil*, Suresh Govindarajalu*, Mark Dzietko*, Stefanie Pesditschek*, Ingrid Mai†, Krikor Dikranian‡, John W. Olney‡, and Chrysanthy Ikonomidou*§

*Department of Pediatric Neurology, Children's Hospital, Charite-Virchow Clinics, Humboldt University, Augustenburger Platz 1, 13353 Berlin, Germany; †Department of Clinical Pharmacology, Humboldt University, Schumannstrasse 20/21, 10117 Berlin, Germany; and ‡Department of Psychiatry, Washington University School of Medicine, 4940 Children's Place, St. Louis, MO 63110

Epilepsy is the most common neurological disorder of young humans. Each year 150,000 children in the United States experience their first seizure. Antiepileptic drugs (AEDs), used to treat seizures in children, infants, and pregnant women, cause cognitive impairment, microcephaly, and birth defects. The cause of unwanted effects of therapy with AEDs is unknown. Here we reveal that phenytoin, phenobarbital, diazepam, clonazepam, vigabatrin, and valproate cause apoptotic neurodegeneration in the developing rat brain at plasma concentrations relevant for seizure control in humans. Neuronal death is associated with reduced expression of neurotrophins and decreased concentrations of survival-promoting proteins in the brain. β-Estradiol, which stimulates pathways that are activated by neurotrophins, ameliorates AED-induced apoptotic neurodegeneration. Our findings present one possible mechanism to explain cognitive impairment and reduced brain mass associated with prenatal or postnatal exposure of humans to antiepileptic therapy.

survival | epilepsy | rat | neurotrophins

A seizure is a sudden change in behavior caused by synchronous, rhythmic firing of neurons in the brain. Between 2% and 4% of all children in Europe and the United States experience at least one seizure before the age of 5 years (1). Epilepsy, a brain disorder characterized by recurrent seizures, affects 1–2% of humans worldwide and shows its highest incidence in the first year of life (1).

Antiepileptic drugs (AEDs) are used to prevent or interrupt seizures. They act via three mechanisms: (*i*) limitation of sustained repetitive neuronal firing via blockade of voltage-dependent sodium channels; (*ii*) enhancement of γ-aminobutyric acid (GABA)-mediated inhibition; and (*iii*) blockade of glutamatergic excitatory neurotransmission (2–5). Phenytoin decreases neuronal firing through use-dependent blockade of voltage-gated sodium channels. Barbiturates and benzodiazepines enhance inhibition in the brain by allosterically modulating permeability of the chloride channel coupled to the GABA type A receptor. Vigabatrin decreases GABA breakdown by blocking the GABA-degrading enzyme GABA transaminase, and valproate influences GABA synthesis and breakdown, leading to an increase of GABA concentrations in the brain. Valproate also interferes with glutamate-mediated excitation and limits sustained repetitive neuronal firing through voltage- and use-dependent blockade of sodium channels (2–5).

AEDs are among the most common causes of fetal malformations, developmental delay, and microcephaly (6–11). Increasing maternal blood levels and combinations of AEDs impose an increased risk for harm to human infants (11). AEDs may also exert unfavorable effects on human intellect when given to treat seizures in infants and toddlers. Therapy with barbiturates during the first 3 years of life may cause cognitive impairment that persists into adulthood (12–16). Although neurotoxic effects of AEDs have been recognized since the 1970s, the underlying mechanisms are not understood.

In the immature rodent brain, suppression of synaptic neurotransmission via blockade of glutamate *N*-methyl-D-aspartate receptors or activation of GABA type A receptors may trigger apoptotic neurodegeneration (17, 18). Because depression of synaptic neurotransmission is the common denominator in the action of AEDs, we investigated whether common AEDs may cause apoptotic neurodegeneration in the developing brain and what the underlying pathogenetic mechanisms are. Furthermore, we attempted to identify measures that will prevent AED neurotoxicity.

Materials and Methods

***In Vivo* Experiments.** Wistar rats (Bundesinstitut für gesundheitlichen Verbraucherschutz und Veterinärmedizin, Berlin), 0–30 days old, received i.p. administration of AEDs, β-estradiol, or vehicle (normal saline) and were allowed to survive for up to 48 h after injection.

The following drugs and doses were administered: phenytoin (Desitin, Hamburg, Germany), 10–50 mg/kg; phenobarbital (Desitin), 20–100 mg/kg; pentobarbital (Sigma), 5 and 10 mg/kg; diazepam (Ratiopharm, Ulm, Germany), 5–30 mg/kg; clonazepam (Desitin), 0.5–4 mg/kg; valproate (Sigma), 50–400 mg/kg; and vigabatrin (Aventis, Bad Soden, Germany), 50, 100, or 200 mg/kg twice daily on 3 consecutive days. Flumazenil (Hoffman–La Roche) was administered in hourly intervals for 5 h at the dose of 2 mg/kg, beginning 15 min after administration of diazepam (30 mg/kg) or clonazepam (4 mg/kg). β-Estradiol (Sigma) was administered three times at the dose of 300 μg/kg every 8 h.

Intracerebroventricular injections of U0126 (Calbiochem) or wortmannin (Calbiochem) were performed in pups subjected to brief halothane anesthesia by using a Hamilton syringe with a 27-gauge needle. The location was 1 mm rostral, 1.5 mm lateral to bregma, and 2 mm deep to skull surface. Drugs were dissolved in 10% DMSO and phosphate buffer and administered in a volume of 1 μl over 2 min. Control pups received i.c.v. injection of vehicle.

To exclude the possibility that hypoxia might contribute to histological changes detected in the brains, oxygen saturations were measured every 30 min over a period of 4 h after injection of the drugs by pulse oximetry.

At the end of the observation period, animals received an overdose of chloralhydrate (150 mg/kg). Before perfusion fixation, a 200-μl blood sample was obtained from the left ventricle for measurement of drug-plasma concentrations. Rats were perfused through the heart and ascending aorta for 15 min with a solution containing paraformaldehyde (1%) and glutaraldehyde (1.5%) in pyrophosphate buffer (for combined light and electron microscopy) or paraformaldehyde (4%) in cacodylate buffer (for terminal deoxynucleotidyltransferase-mediated dUTP end labeling or De-Olmos cupric silver staining).

Histology. To visualize degenerating cells, coronal sections of the whole brain were stained with silver nitrate and cupric nitrate (19).

MEDICAL SCIENCES

Table 1. Phenytoin, phenobarbital, and valproate increase the rate of apoptosis in the brain of 7-day-old rats

	Vehicle		Phenytoin	Phenobarbital	Valproate
Brain region	Numerical density of total cells, mean/mm^3 ± SEM	Degenerating cells as % of total cells, mean ± SEM	Degenerating cells as % of total cells, mean ± SEM	Degenerating cells as % of total cells, mean ± SEM	Degenerating cells as % of total cells, mean ± SEM
CA1 HC	220,050 ± 4,584	0.85 ± 0.11	2.63 ± 0.43*	2.09 ± 0.45*	1.97 ± 0.40*
DG	284,127 ± 23,089	0.37 ± 0.06	1.21 ± 0.14***	1.54 ± 0.11***	1.32 ± 0.20**
Subiculum	198,124 ± 8,205	0.59 ± 0.04	2.28 ± 0.31***	3.79 ± 0.41***	7.30 ± 0.51***
Caudate	242,534 ± 11,140	0.29 ± 0.04	0.58 ± 0.04**	1.81 ± 0.29***	2.17 ± 0.16***
Thal LD	133,945 ± 13,148	0.30 ± 0.05	2.62 ± 0.37***	9.94 ± 0.96***	15.90 ± 3.53***
Thal MD	199,335 ± 6,398	0.40 ± 0.01	1.86 ± 0.34**	3.33 ± 0.79***	6.39 ± 1.57**
Thal V	132,907 ± 2,634	0.76 ± 0.05	0.72 ± 0.20ns	1.39 ± 0.21*	4.47 ± 0.97**
Hth VM	134,500 ± 2,343	0.90 ± 0.01	2.16 ± 0.15***	2.72 ± 0.51***	6.88 ± 0.90**
Fr II	219,432 ± 4,541	1.55 ± 0.18	5.19 ± 0.38***	4.23 ± 0.32***	4.64 ± 0.14***
Fr IV	142,120 ± 10,323	0.20 ± 0.05	2.57 ± 0.21***	1.46 ± 0.21***	3.33 ± 0.55***
Par II	223,900 ± 13,434	1.08 ± 0.28	6.07 ± 0.64***	4.01 ± 0.50***	4.22 ± 0.19***
Par IV	156,078 ± 6,323	0.22 ± 0.05	3.31 ± 0.33***	1.54 ± 0.29**	2.36 ± 0.49**
Cing II	218,932 ± 11,239	1.54 ± 0.21	3.59 ± 0.56**	4.80 ± 0.45***	3.01 ± 0.51**
Cing IV	148,100 ± 6,125	0.13 ± 0.03	2.85 ± 0.32***	1.15 ± 0.69*	6.01 ± 0.81***
Rspl II	235,948 ± 13,857	0.89 ± 0.07	2.16 ± 0.07***	1.78 ± 0.19***	1.40 ± 0.14**
Rspl IV	143,250 ± 10,857	0.33 ± 0.08	3.06 ± 0.22***	1.38 ± 0.21*	4.52 ± 0.64***

Rats received vehicle, phenytoin (50 mg/kg), phenobarbital (75 mg/kg), or valproate (400 mg/kg) and were killed 24 h later on P8. Using an optical disector method the numerical densities of total cells (cells per mm^3) and degenerating cells (degenerating cells per mm^3) in 16 brain regions of vehicle- ($n = 6$), phenytoin- ($n = 6$), phenobarbital- ($n = 6$), and valproate-treated rats ($n = 6$) were estimated. In column 2, mean numerical total cell densities ± SEM in 8-day-old rats are shown. The extent of apoptosis in vehicle-, phenytoin-, phenobarbital-, and valproate-treated rats is shown as the ratio of degenerating cell density to total cell density and is presented as % ± SEM. *, $P < 0.05$; **, $P < 0.01$; ***, $P < 0.001$, Student's t test. CA1 HC, CA1 hippocampus; DG, dentate gyrus; Thal, thalamus; LD, laterodorsal; MD, mediodorsal; V, ventral; Hthal VM, ventromedial hypothalamus; Fr, frontal cortex; Par, parietal cortex; Cing, cingulate cortex; Rspl, retrosplenial cortex; II, IV, cortical layers 2 and 4.

To visualize nuclei with DNA cleavage, serial coronal paraffin sections (10 μm) of the entire brain were cut on a microtome and residues of peroxidase-labeled digoxigenin nucleotides were catalytically added to DNA fragments by terminal deoxynucleotidyltransferase (TdT Frag EL, DNA Fragmentation Detection Kit, Calbiochem-Novabiochem).

For light microscopy on plastic sections and electron microscopy brains were sliced in 1-mm thick slabs, fixed in osmium tetroxide, dehydrated in alcohols, and embedded in araldite. Ultrathin sections were cut and stained with uranyl acetate/lead citrate.

Quantitation. Quantitation of damage was performed in silver-stained sections by estimating mean numerical densities (N_v) of degenerating cells (20). An unbiased counting frame (0.05 mm × 0.05 mm; disector height 0.07 mm) and a high aperture objective were used for the sampling. Counts were performed in a blinded manner. N_v values from 16 brain regions (Table 1) were summed to give a total score for degenerating neurons for each brain.

RT-PCR Studies and Western Blotting. Total cellular RNA was isolated from snap-frozen tissue by acidic phenol/chloroform extraction and DNase treatment (Hybaid, Roche Diagnostics); 500 ng of RNA was reverse-transcribed with Moloney murine leukemia virus reverse transcriptase (Promega) and oligo(dT)$_{16}$ primer (Roche Diagnostics) in 25 μl of reaction mixture. cDNA (1 μl) was amplified by PCR in 30 cycles, subjected to PAGE, subsequent silver staining, and densitometric analysis with the image analysis program BIODOCANALYZE (Whatman Biometra). Primers for brain-derived neurotrophic factor (BDNF) [Gen-Bank accession no. D10938; sense, 5′-CGACGTCCCTGGCTG-GACACTTTT-3′ (positions 2296–2318); and antisense 5′-AGTAAGGGCCCGAACATACGATTGG-3′ (positions 2762–2786)], primers for neurotrophin 3 (NT-3) [GenBank accession no. M34643,; sense, 5′-GGTCAGAATTCCAGCCGATGATTGC-3′ (positions 308–332); and antisense 5′-CAGCGCCAGCCTAC-GAGTTTGTTGT-3′ (positions 767–791)], and primers for β-actin [GenBank accession no. V01217; sense, 5′-CCCTAAGGCCAAC-CGTGAAAAGATG-3′ (positions 1663–1687); and antisense 5′-GAACCGCTCATTGCCGATAGTGATG-3′ (positions 2535–2559)], were used.

For Western blotting analysis of brain tissue, animals were killed, and brains were removed, microdissected, and then immediately snap-frozen in liquid nitrogen.

Tissue was then homogenized at 4°C in a Tris·HCL buffer (50 mM, pH 7.6). Homogenate was centrifuged at 15,000 × g for 20 min, and the supernatant was used as the cytosolic fraction.

Total cellular proteins (30 μg/lane cytosolic fraction) were separated on a 10% SDS-polyacrylamide gel and electrotransferred onto nitrocellulose membranes (Hybond ECL, Amersham Pharmacia). The membranes were incubated overnight at 4°C with the following antibodies: antiphospho-raf (1:2,000), antiphospho-ERK1/2 (1:2,000), antiphospho-AKT (1:2,000), anti-ERK1/2 phosphorylation state independent (1:2,000), or anti-AKT phosphorylation state independent (1:2,000) (Cell Signaling Technology, Beverly, MA). After incubation with secondary antibody conjugated to horseradish peroxidase (anti-mouse, 1:1,000 dilution), immunoreactive proteins were detected by the enhanced chemiluminescence system (ECL, Amersham Pharmacia) and serial exposures were made to radiographic film (Hyperfilm ECL, Amersham Pharmacia). Densitometric analysis of the blots was performed with the image analysis program TINA 2.09g.

Results

To determine whether AEDs exert neurotoxic effects in the developing rat brain, we injected rats i.p. with phenytoin, phenobarbital, pentobarbital, diazepam, clonazepam, vigabatrin, or valproate on postnatal day 7 (P7) and analyzed their brains 24 h later.

In the brains of vehicle-treated rats, either silver or terminal deoxynucleotidyltransferase-mediated dUTP end labeling revealed a light pattern of neurodegeneration attributable to programmed cell death (21) (Table 1).

Phenytoin (10–50 mg/kg) produced widespread neurodegeneration on P7 (Fig. 1, Table 1). By electron microscopy it was determined that the cells degenerating in the brains of phenytoin-treated rats displayed ultrastructural changes similar to those described in neurons undergoing programmed cell death (21). A
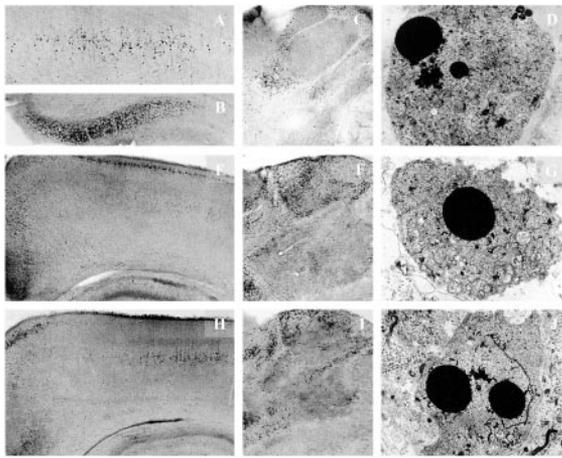
Fig. 1. Light microscopic overviews of silver-stained transverse sections and electron micrographs depicting neurodegenerative changes in the brains of P8 rats after treatment with phenytoin (*A–D*), diazepam (*E–G*), or valproate (*H–J*). (*A–C*) Layer IV of the parietal cortex (*A*, ×40), the subiculum (*B*, ×40), and the thalamus (*C*, ×25) of P8 rats treated 24 h previously with phenytoin (50 mg/kg). (*E* and *F*) Low-magnification (×25) light microscopic overviews of silver-stained sections from the parietal and cingulate cortices (*E*) and the thalamus (*F*) of P8 rats treated 24 h previously with diazepam (30 mg/kg). (*H* and *I*) Low-magnification (×25) light microscopic overviews of silver-stained sections from the parietal and cingulate cortices (*H*) and the thalamus (*I*) of P8 rats treated 24 h previously with valproate (200 mg/kg). Degenerating neurons (small dark dots) are sparsely present after treatment with saline in those same brain regions but abundantly present after treatment with phenytoin, diazepam, or valproate. (*D*, *G*, and *J*) Electron micrographs (×1,800) illustrating late stages of apoptotic neurodegeneration within the thalamus 24 h after administration of phenytoin (*D*), diazepam (*G*), or valproate (*J*) to rats on P7.

proapoptotic effect of phenytoin has been described in the developing mouse cerebellum (22).

Phenytoin's neurotoxic action in the forebrain was dose-dependent. The threshold dose was 20 mg/kg, which resulted in phenytoin plasma concentrations ranging between 10 and 15 μg/ml over 4 h (Fig. 2).

Phenobarbital (20–100 mg/kg) and diazepam (5–30 mg/kg) caused widespread apoptotic neurodegeneration in the brains of rats on P7 (Fig. 1, Table 1). By electron microscopy (Fig. 1) it was determined that the cells degenerating in the brains of phenobarbital- or diazepam-treated rats fulfilled ultrastructural criteria for apoptosis. Neurotoxic effects were reproduced by pentobarbital (5 or 10 mg/kg) and clonazepam (0.5–4 mg/kg) in 7-day-old rats. Administration of the benzodiazepine receptor antagonist flumazenil prevented apoptotic neurodegeneration induced by diazepam (data not shown).

The threshold doses for triggering apoptotic brain damage were 40 mg/kg for phenobarbital, 10 mg/kg for diazepam, and 0.5 mg/kg for clonazepam (Fig. 2). These doses caused sedation but no hypoxia or cardiorespiratory compromise in 7-day-old rats. When concentrations of phenobarbital were maintained at 25–35 μg/ml over a 12-h period significant apoptotic neurodegeneration occurred (Fig. 2).

Valproate (50–400 mg/kg on P7) or vigabatrin (50, 100, or 200 mg/kg twice daily on 3 consecutive days starting on P5) elicited apoptotic neurodegeneration in the developing rat brain in a dose-dependent manner (Figs. 1 and 2, Table 2). The threshold dose for valproate was 50 mg/kg (Fig. 2) and resulted in a peak valproate plasma concentration of 80 μg/ml, which rapidly declined within 8 h. The threshold dose for vigabatrin was 100 mg/kg given twice daily on 3 consecutive days.

To investigate whether a combination of AEDs with different modes of action may result in a more profound neurodegenerative
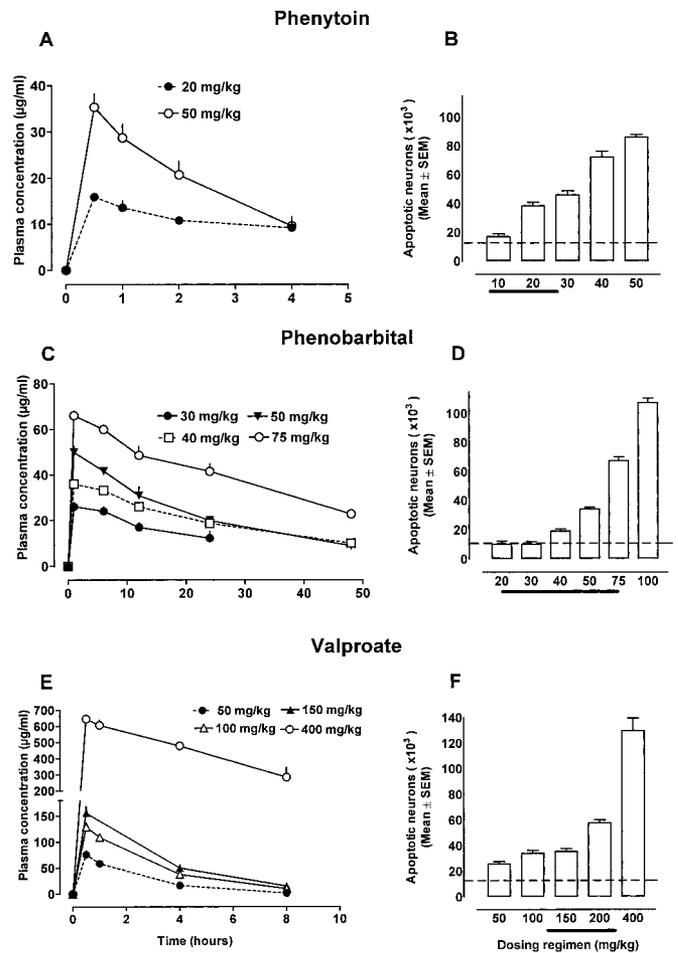
Fig. 2. Phenytoin (10–50 mg/kg), phenobarbital (30–75 mg/kg), or valproate (50–400 mg/kg) were administered to P7 rats. (*A*, *C*, and *E*) Phenytoin, phenobarbital, and valproate plasma concentrations associated with each of the several dosing regimens. Dotted lines represent threshold levels for triggering an apoptotic response. (*B*, *D*, and *F*) Severity of apoptotic neurodegeneration associated with each dose-plasma concentration curve. Severity of degeneration was established as described in *Materials and Methods*. Histographic values in *B*, *D*, and *F* represent cumulative scores for apoptotic brain damage (means ± SEM, $n = 6$ per group) in the forebrains of treated rats. Dotted lines in *B*, *D*, and *F* represent the mean score for apoptotic neurons in saline-treated rats. ANOVA revealed a significant effect of treatment with phenytoin [$F_{(1,50)} = 703.8$, $P < 0.0001$], phenobarbital [$F_{(1,60)} = 555.1$, $P < 0.0001$], and valproate [$F_{(1,50)} = 356.0$, $P < 0.0001$] with multiple comparisons showing that the doses of 20 mg/kg phenytoin, 40 mg/kg phenobarbital, and 50 mg/kg valproate significantly increased apoptosis. Thick lines at the x coordinate indicate reported ED$_{50}$ doses of the corresponding drug in various rodent seizure models. ED$_{50}$ is defined as the dose that blocks seizures in 50% of tested animals.

response compared with monotherapy, we administered diazepam (5 mg/kg) in combination with phenobarbital (20 mg/kg) or phenytoin (20 mg/kg) to rats on P7. This combination resulted in profound apoptotic neurodegeneration with the combination of diazepam and phenobarbital being most detrimental (Fig. 3). Oxygen saturations remained above 90% in pups treated with phenobarbital and diazepam.

To determine whether treatment with AEDs causes a persistent reduction in brain weight, we administered a single dose of phenytoin (50 mg/kg, $n = 6$), phenobarbital (75 mg/kg, $n = 6$), or valproate (300 mg/kg, $n = 6$) to P7 rats and measured unperfused hemispheric brain weights after 8 days. A single treatment with phenytoin on P7 led to a significant decrease in mean hemispheric weight of 9.2% (0.3958 ± 0.008 g vs. 0.4363 ± 0.03 g in vehicle-

Table 2. Phenobarbital, valproate, and vigabatrin trigger an increased rate of apoptosis in the rat brain on P0, P3, or P7

Numerical density of degenerating neurons, means/mm³ ± SEM

Brain region	P0					P3					P7						
	Vehicle	Phenobarbital	Fold↑	Valproate	Fold↑	Vehicle	Phenobarbital	Fold↑	Valproate	Fold↑	Vehicle	Phenobarbital	Fold↑	Valproate	Fold↑	Vigabatrin	Fold↑
CA1 HC	3,789 ± 305	5,867 ± 892	1.6	5,333 ± 893	1.4	4,576 ± 756	6,318 ± 715	1.4	4,877 ± 243	1.1	1,863 ± 242	4,599* ± 990	2.5	4,335* ± 880	2.3	1,968** ± 340	1.1
DG	4,796 ± 716	5,333 ± 337	1.1	8,533** ± 892	1.8	2,745 ± 420	3,095 ± 538	1.1	3,365 ± 208	1.2	1,045 ± 170	4,376** ± 313	4.2	3,750** ± 568	3.5	1,905** ± 142	1.8
Subiculum	3,996 ± 459	9,600*** ± 587	2.4	26,755** ± 5,635	6.7	3,663 ± 760	12,374** ± 2,611	3.4	6,832* ± 844	1.9	1,168 ± 172	7,509*** ± 812	6.4	14,463*** ± 1,010	12.4	3,448** ± 890	3.0
Caudate	8,349 ± 915	8,400 ± 1,168	1.0	11,467* ± 447	1.4	4,359 ± 740	5,125 ± 226	1.2	4,960 ± 198	1.1	703 ± 97	4,310*** ± 388	6.1	5,263*** ± 388	7.5	1,028** ± 99	1.5
Hypothal vm	23,186 ± 2,309	24,000 ± 2,800	1.0	25,066 ± 2,361	1.1	1,835 ± 270	6,498*** ± 715	3.5	7,131*** ± 880	3.9	1,209 ± 14	3,658** ± 686	3.0	9,254** ± 1,211	7.6	4,686** ± 851	3.9
Thal ld	2,428 ± 423	11,733*** ± 1,687	4.8	11,945** ± 2,115	4.9	3,172 ± 756	23,265*** ± 4,583	7.3	10,104** ± 1,599	3.2	402 ± 67	13,310*** ± 962	33.0	10,150*** ± 2,433	25.2	1,486** ± 147	3.7
Thal md	18,824 ± 2,078	19,333 ± 2,264	1.0	30,667** ± 4,088	1.6	926 ± 85	8,406*** ± 1,476	9.6	9,554** ± 1,281	10.3	768 ± 20	6,578** ± 1,574	8.6	12,738** ± 2,731	16.6	3,886*** ± 610	5.1
Thal v	10,787 ± 693	19,733*** ± 1,470	1.8	21,333*** ± 892	2.0	1,156 ± 205	4,138** ± 663	3.6	2,920*** ± 230	2.5	1,003 ± 66	1,847** ± 279	1.8	5,941** ± 1,289	5.9	1,600** ± 140	1.6
Fr II	0	0 (–)	(–)	0 (–)	(–)	5,672 ± 750	10,123** ± 822	1.8	5,932 ± 419	1.1	3,398 ± 395	9,282*** ± 702	2.7	10,182** ± 307	3.0	5,016* ± 512	1.5
Par II	0	0 (–)	(–)	0 (–)	(–)	5,291 ± 905	8,088 ± 914	1.5	7,741 ± 527	1.5	2,421 ± 602	8,978*** ± 1,170	3.7	9,448*** ± 425	3.9	5,397** ± 526	2.3
Cing II	0	0 (–)	(–)	0 (–)	(–)	9,242 ± 1,200	11,308 ± 748	1.2	10,595 ± 1,028	1.2	3,369 ± 445	10,509*** ± 985	3.2	6,570** ± 1,117	2.0	5,853** ± 344	1.7
Cing IV	0	0 (–)	(–)	0 (–)	(–)	3,065 ± 518	4,127 ± 395	1.4	4,001 ± 415	1.3	196 ± 44	1,700*** ± 132	8.67	1,693** ± 282	8.63	2,223** ± 511	11.3
Rspl II	0	0 (–)	(–)	0 (–)	(–)	5,320 ± 445	6,104 ± 276	1.2	7,467* ± 692	1.4	2,089 ± 159	4,200** ± 448	2.0	3,303** ± 330	1.6	2,647*** ± 366	1.3
Rspl IV	0	0 (–)	(–)	0 (–)	(–)	2,104 ± 482	2,575 ± 240	1.2	2,857 ± 370	1.4	476 ± 115	1,975** ± 193	4.1	3,006*** ± 809	6.3	1,079*** ± 55	2.3

At these ages rat pups received vehicle, 75 mg/kg phenobarbital i.p., or 400 mg/kg valproate at 0 h and were killed at 24 h. Vigabatrin was administered at the dose of 400 mg/kg on 3 subsequent days, starting on P5, and the pups were perfused on P8 (24 h after the last dose). Using an optical disector method (20), the numerical densities of degenerating neurons (degenerating neurons per mm³) in 14 brain regions of vehicle and drug-treated pups were estimated. Shown are mean numerical densities of degenerating neurons ± SEM ($n = 6$). Effects of phenobarbital, valproate, and vigabatrin on the rate of apoptosis at each age are presented as ratios of mean numerical densities of degenerating cells in drug-treated vs. age-matched vehicle-treated rats (expressed as fold ↑). Note that both phenobarbital and valproate do not trigger apoptosis in brain regions displaying no physiological apoptosis and that vulnerability to their proapoptotic action depends on developmental age. *, $P < 0.05$; **, $P < 0.01$; ***, $P < 0.001$, Student's t test. Abbreviations are as in Table 1.
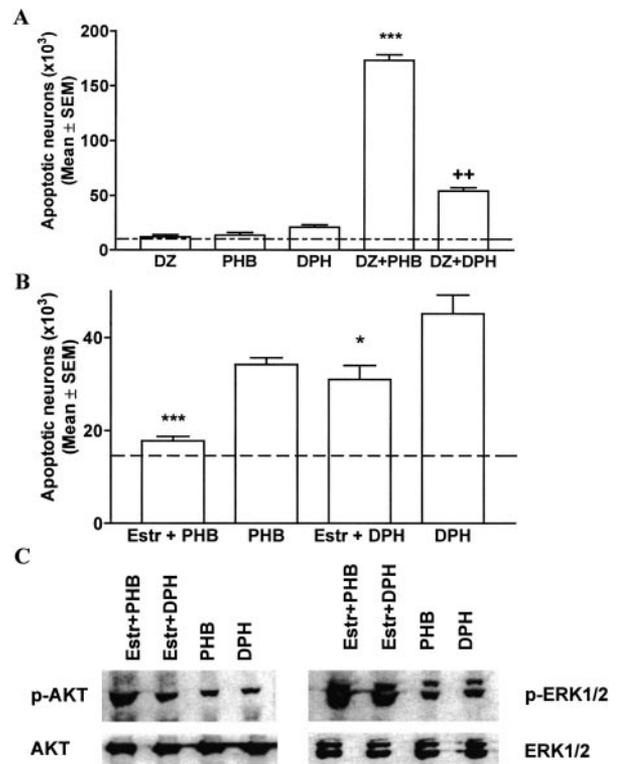
Fig. 3. (*A*) Combinations of AEDs elicit neurotoxic effects. Diazepam (DZ, 5 mg/kg), phenobarbital (PHB, 20 mg/kg), and phenytoin (DPH, 20 mg/kg) were administered alone or in combination to P7 rats. Severity of degeneration was established as described in *Materials and Methods*. Histographic values represent cumulative scores for apoptotic damage (means ± SEM, $n = 6$ per group) in the forebrains of treated rats on P8. Dotted line represents the mean apoptotic score in saline-treated rats. Whereas these doses of AEDs alone elicited no or minimal neurotoxic response, their combination resulted in severe apoptotic neurodegeneration (***, $P < 0.001$ compared with DZ- and PHB-treated rats; ††, $P < 0.01$ compared with DPH-treated rats, Student's t test. (*B*) β-Estradiol (Estr) ameliorates apoptotic response to phenobarbital (PHB) and phenytoin in P7 rats. Saline or β-estradiol (300 µg/kg) were administered s.c. to P6 rats in three injections 8 h apart. Pups received i.p. injection of phenobarbital (50 mg/kg) or phenytoin (30 mg/kg) on P7 and the brains were analyzed on P8. Histographic values represent cumulative scores for brain damage (means ± SEM, $n = 6$ per group) in the forebrains of treated rats on P8. The scores illustrate that there are fewer apoptotic neurons in the brains of β-estradiol-treated rats compared with saline-treated rats (***, $P < 0.001$ for phenobarbital; *, $P < 0.05$ for phenytoin, Student's t test). (*C*) β-Estradiol increases protein levels for p-ERK1/2 and p-AKT but does not alter total protein levels in the thalamus of rats treated with phenobarbital (50 mg/kg) or phenytoin (50 mg/kg). Immunoblotting was performed with antiphospho-ERK1/2, antiphospho-AKT, ERK1/2 (phosphorylation state independent), or AKT (phosphorylation state independent) antibodies. Blots are representative of a series of four blots for each antibody and each treatment condition.

treated rats, $P < 0.05$). Phenobarbital treatment also resulted in a significant decrease in hemispheric weight of 8% (0.4012 ± 0.008 g, $P < 0.05$). Similarly, valproate treatment resulted in a decrease of hemispheric weight of 15% compared with control rats (0.3698 ± 0.01g, $P < 0.001$).

To determine how the apoptotic response to AEDs might differ as a function of developmental age, we administered either saline, phenobarbital (75 mg/kg), or valproate (400 mg/kg) to postnatal rats on P0, P3, P7, P14, and P20. These experiments revealed (Table 2) that there is a time window from P0 to P14 when various neuronal populations in the forebrain show transient sensitivity to phenobarbital and valproate, and within this period, different neuronal populations display transient sensitivity at different times (Table 2).

Neurotrophins provide trophic support to developing neurons and their withdrawal may lead to neuronal death (23). We tested

Fig. 4. (*A*) Phenobarbital and phenytoin decrease mRNA levels for BDNF and NT-3 and decrease phosphorylation of c-RAF, ERK1/2, and AKT in the neonatal brain. P7 pups received i.p. injection of phenobarbital (50 mg/kg), phenytoin (40 mg/kg), or vehicle (Co). Brain tissue from the thalamus was dissected at the various times indicated. Decreased density of the BDNF- and NT-3-specific bands is evident at 6, 12, and 24 h after administration of AEDs. Immunoblotting was performed with antiphospho-RAF, antiphospho-ERK1/2, antiphospho-AKT, ERK1/2 (phosphorylation state independent), or AKT (phosphorylation state independent) antibodies. There is a decrease in the levels of p-RAF, p-ERK1/2, and p-AKT at 6 h after injection of AEDs, whereas ERK1/2 and AKT (phosphorylation independent) are unaffected. (*B*) Quantitation of suppression by AEDs of mRNA levels for BDNF and NT-3 in the thalamus of infant rats. P7 pups received injection of phenobarbital (50 mg/kg, $n = 9$), phenytoin (50 mg/kg, $n = 9$), valproate (200 mg/kg, $n = 9$), or vehicle ($n = 9$) and were killed at 6, 12, or 24 h after treatment ($n = 3$ per group). mRNA levels for BDNF, NT-3, and β-actin were analyzed by means of PAGE and densitometrically quantitated. Values represent mean normalized ratios of the BDNF and NT-3 bands to β-actin ($n = 3$ per point $\pm$ SEM). ANOVA revealed that there was a significant effect of treatment
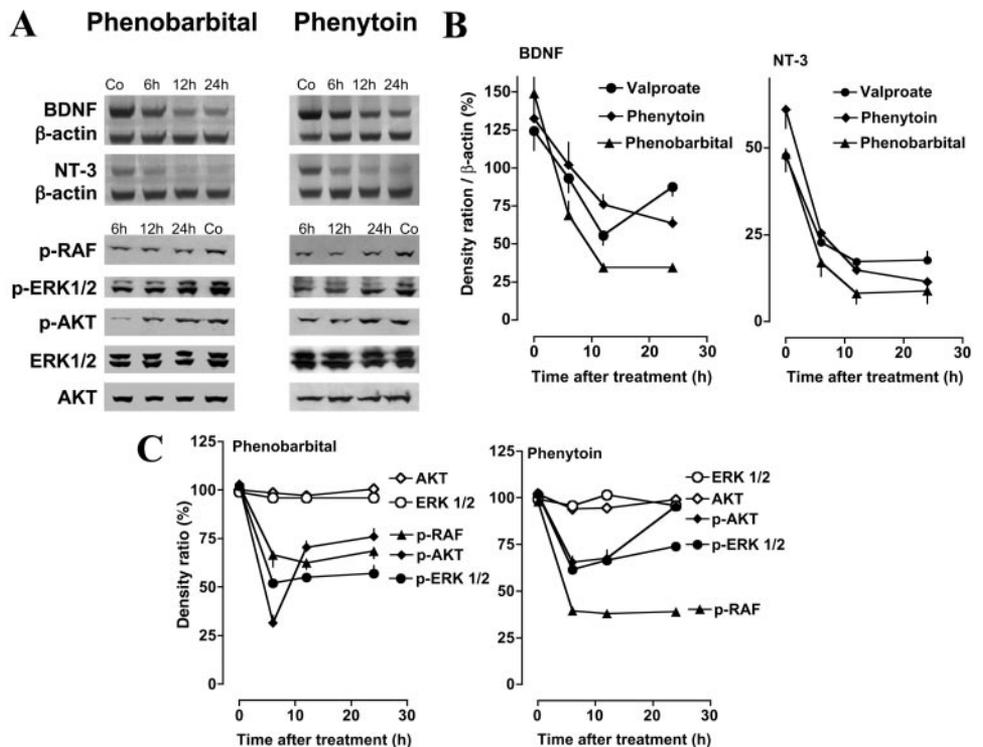
with AEDs on BDNF [$F_{(1,12)\text{valproate}} = 29.79$, $P < 0.0001$; $F_{(1,12)\text{phenytoin}} = 5.492$, $P < 0.05$; $F_{(1,12)\text{phenobarbital}} = 838.2$, $P < 0.0001$] and NT-3 [$F_{(1,12)\text{valproate}} = 283.9$, $P < 0.0001$; $F_{(1,12)\text{phenytoin}} = 167.3$, $P < 0.0001$; $F_{(1,12)\text{phenobarbital}} = 109.2$, $P < 0.0001$] levels. (*C*) Quantitation of suppression by AEDs of protein levels of p-RAF, p-ERK1/2, and p-AKT in the thalamus of infant rats. P7 pups received injection of phenobarbital (50 mg/kg, $n = 16$), phenytoin (50 mg/kg, $n = 16$), or vehicle ($n = 16$) and were killed at 0, 6, 12, or 24 h after treatment ($n = 4$ per group). Protein levels for p-RAF, p-ERK1/2, p-AKT, ERK1/2, and AKT were analyzed by Western blotting and densitometrically quantitated. Values represent the mean normalized values of the densities of p-RAF, p-ERK1/2, p-AKT, ERK1/2, and AKT bands compared with the density of the respective band at 0 h (percent; $n = 4$ per point $\pm$ SEM). ANOVA revealed that there was a significant effect of treatment with AEDs on p-RAF [$F_{(1,24)\text{phenobarbital}} = 115.9$, $P < 0.0001$; $F_{(1,24)\text{phenytoin}} = 3,206$, $P < 0.0001$], p-ERK1/2 [$F_{(1,24)\text{phenobarbital}} = 477.4$, $P < 0.0001$; $F_{(1,24)\text{phenytoin}} = 478.7$, $P < 0.0001$] and p-AKT [$F_{(1,24)\text{phenobarbital}} = 254.3$, $P < 0.0001$; $F_{(1,24)\text{phenytoin}} = 96.69$, $P < 0.0001$] levels. ERK1/2 and AKT levels were not affected by treatment.

whether and how AEDs affect expression of the neurotrophins BDNF and NT-3 in the cingulate cortex, hippocampus, and thalamus in P7 rats. Phenobarbital (50 mg/kg), valproate (200 mg/kg), and phenytoin (40 mg/kg) reduced mRNA levels for BDNF and NT-3, as revealed by RT-PCR analysis, in all three areas. This down-regulation was evident within 6 h and still present at 24 h after administration of the AEDs (Fig. 4).

Western blot analysis revealed decreased levels of the active, phosphorylated isoforms of the serine-threonin kinase AKT (p-AKT, protein kinase B), and the members of the mitogen-activated protein kinase pathway c-RAF and extracellular signal-related protein kinase ERK1/2 (p-ERK1/2), which mediate intracellular signaling after activation of receptor tyrosine kinases by growth factors (Fig. 4) (24).

To confirm that reduction of levels of phosphorylated forms of ERK1/2 and AKT may cause neurodegeneration in the developing rat brain, we injected the mitogen-activated protein kinase kinase inhibitor U0126 (2 nmol), the phosphatidylinositol 3-kinase inhibitor wortmannin (2 nmol), or vehicle into the right cerebral ventricle of P7 rats and analyzed the brains 24 h later for signs of degeneration. These doses of U0126 and wortmannin have been shown to reduce p-ERK1/2 and p-AKT levels in the brains of P7 rats (25). Both compounds induced a significant neurodegenerative response in brain areas surrounding the right cerebral ventricle, i.e., septum and caudate nucleus.

The female hormone estrogen has neuroprotective properties in models of *in vitro* and *in vivo* neurodegeneration. These properties result from activation of estrogen receptors and cross-talking of estrogen with intracellular signaling pathways that are activated by neurotrophins, such as mitogen-activated protein kinase and phos-

phatidylinositol 3-AKT pathways (26). In an attempt to identify measures that will counteract neurotoxicity of AEDs and taking into consideration that AEDs impair neurotrophin-activated signaling, we investigated whether stimulation of these same pathways by β-estradiol may ameliorate phenobarbital- and phenytoin-induced apoptotic neurodegeneration.

β-Estradiol (total of three injections at 300 μg/kg every 8 h starting 10 h before the injection of phenobarbital or phenytoin) or vehicle were injected s.c. to P7 rats followed by phenobarbital (50 mg/kg) or phenytoin (30 mg/kg) on P7.

The numerical densities of degenerating cells in 16 evaluated brain regions were significantly lower in β-estradiol-pretreated pups in comparison to P7 pups who received phenobarbital, phenytoin, and vehicle (Fig. 3*B*). Analysis of protein levels for p-AKT and p-ERK1/2 revealed higher levels for p-AKT and p-ERK1/2 after β-estradiol treatment (Fig. 3*C*).

Discussion

Here we report that major AEDs cause sensitive neurons to undergo apoptotic death in the developing rat forebrain. These findings apply to compounds that block voltage-gated sodium channels, enhance GABAergic inhibition, or block glutamate-mediated excitation. Neurotoxicity of AEDs is age-dependent and is associated with impairment of neurotrophin-mediated, survival-promoting signals in the brain. The combination of AEDs with different modes of action results in a substantially higher apoptotic response compared with monotherapy.

Proapoptotic threshold doses and plasma concentrations of AEDs are not higher than their reported anticonvulsant doses in rodent seizure models. ED_{50} doses range between 5 and 25 mg/kg

MEDICAL SCIENCES

Bittigau *et al.*

for phenytoin (27, 28), 5 and 15 mg/kg for diazepam, and 0.4 and 0.6 mg/kg for clonazepam (28–31). We found that phenobarbital plasma concentrations between 25 and 35 μg/ml over a 12-h period triggered apoptotic neurodegeneration in infant rats. Such plasma concentrations are easily achieved when phenobarbital is given to human infants for management of seizures or status epilepticus and in the course of long-term antiepileptic treatment (32, 33). Reported ED_{50} doses for vigabatrin in rodent seizure models range between 200 and 1,000 mg/kg (34, 35). The threshold neurotoxic dose of valproate (50 mg/kg) was even lower than the reported effective anticonvulsant doses in rodents (133–250 mg/kg). Valproate's high neurotoxicity probably relates to the fact that it acts via several different mechanisms to elicit its anticonvulsant action (3, 4).

We find that AEDs depress an endogenous neuroprotective system in the brain that is crucial for neuronal survival during development (23, 36). Phenytoin, phenobarbital, and valproate depressed synthesis of the neurotrophins BDNF and NT-3 and reduced levels of the active phosphorylated forms of c-RAF, ERK1/2, and AKT. Such changes reflect impairment of survival-promoting signals and an imbalance between neuroprotective and neurodestructive mechanisms in the brain, which, during a developmental period of ongoing programmed neuronal death, will promote apoptotic neurodegeneration (37). In support of this hypothesis, administration of the mitogen-activated protein kinase kinase inhibitor U0126 and the phosphatidylinositol 3-kinase inhibitor wortmannin induced neurodegeneration in the developing rat forebrain. Furthermore, β-estradiol, at doses that increased levels of phosphorylated ERK1/2 and AKT, ameliorated AED neurotoxicity. These findings conform with the hypothesis that depression of the mitogen-activated protein kinase and the phosphatidylinositol 3-AKT pathways by AEDs contributes to the induction of neuronal apoptosis in the developing brain.

The vulnerability period to the proapoptotic effect of AEDs coincides with the brain growth spurt period, which in the rat spans the first 2 postnatal weeks of life (38). In humans, the comparable period begins in the third trimester of gestation and extends to several years after birth. Apoptotic neurodegeneration triggered by AEDs during this critical stage of development can at least partly account for reduced head circumference and impaired intellectual skills observed in prenatally or postnatally exposed humans (6–16). The observation that combinations of AEDs cause more pronounced neurotoxic effects offers one possible explanation for the increased risk for cognitive impairment associated with AED polytherapy (11). It remains open whether other mechanisms, not explored in the context of this study, such as impairment of migration or proliferation of neuronal progenitors as well as disturbance of synaptogenesis, may also account for neurological deficits seen in humans exposed prenatally or postnatally to AEDs.

Our results raise the interesting hypothesis that burst firing may play a role in neuronal survival during critical stages of development. Furthermore, they raise concerns with regard to current clinical practice using AEDs for seizure control in young humans and call for the design of novel AEDs and/or adjunctive neuroprotective therapies that will enable pregnant women, infants, and young children to be safely treated for epilepsy. In addition, measures that promote neurotrophin signaling in the brain may offer a novel adjunctive neuroprotective approach. The finding that β-estradiol ameliorated phenobarbital and phenytoin neurotoxicity is encouraging in that respect. Because the brain growth spurt period in humans begins in the third trimester of gestation, preterm infants, which are prematurely deprived of maternal β-estradiol and are frequently treated with AEDs (especially phenobarbital), are expected to be at high risk for AED neurotoxicity. β-Estradiol replacement therapy in premature infants has been introduced in some centers with the goal to improve bone mineralization (39) and, so far, no adverse side effects have been observed. Based on our findings, we advocate that maintaining *in utero* β-estradiol plasma levels may be one safe and effective measure to protect premature infants from AED neurotoxicity.

1. Hauser, W. A. (1994) *Epilepsia* **35,** Suppl. 2, S1–S6.
2. Taylor, C. P. & Meldrum, B. S. (1995) *Trends Pharmacol. Sci.* **16,** 309–316.
3. Meldrum, B. S. (1996) *Epilepsia* **37,** Suppl. 6, S4–S11.
4. Brodie, M. J. & Dichter, M. A. (1996) *N. Engl. J. Med.* **334,** 168–175.
5. Gidal, B. E., Privitera, M. D., Sheth, R. D. & Gilman, J. T. (1999) *Ann. Pharmacother.* **33,** 1277–1286.
6. Speidel, B. D. & Meadow, S. R. (1972) *Lancet* **308,** 839–843.
7. Strickler, S. M., Dansky, L. V., Miller, M. A., Seni, M. H., Andermann, E. & Spielberg, S. P. (1985) *Lancet* **2,** 746–749.
8. Jones, K. L., Lacro, R. V., Johnson, K. A. & Adams, J. (1989) *N. Engl. J. Med.* **320,** 1661–1666.
9. Buehler, B. A., Delimont, D., Van Waes, M. & Finnel, R. H. (1990) *N. Engl. J. Med.* **322,** 1567–1572.
10. Holmes, L. B., Harvey, E. A., Coull, B. A., Huntington, K. B., Khoshbin, S., Hayes, A. M. & Ryan, L. M. (2001) *N. Engl. J. Med.* **344,** 1132–1138.
11. Zahn, C. A. (1998) *Epilepsia* **39,** Suppl. 8, S26–S31.
12. Farwell, J. R., Lee, Y. J., Hirtz, D. G., Sulzbacher, S. I., Ellenberg, J. H. & Nelson, K. B. (1990) *N. Engl. J. Med.* **322,** 364–369.
13. Reinisch, J. M., Sanders, S. A., Mortensen, E. L. & Rubin, D. B. (1995) *J. Am. Med. Assoc.* **274,** 1518–1525.
14. Sulzbacher, S., Farwell, J. R., Tenkin, N., Lu, A. S. & Hirtz, D. G. (1999) *Clin. Pediatr. (Philadelphia)* **38,** 387–394.
15. Thorp, J. A., O'Connor, M., Jones, A. M., Hoffman, E. L. & Belden, B. (1999) *Am. J. Perinatol.* **16,** 51–60.
16. Dessens, A. B., Cohen-Kettenis, P. T., Mellenbergh, G. J., Koppe, J. G., van De Poll, N. E. & Boer, K. (2000) *Acta Paediatr.* **89,** 533–541.
17. Ikonomidou, C., Bosch, F., Miksa, M., Vöckler, J., Bittigau, P., Dikranian, K., Tenkova, T., Turski, L. & Olney, J. W. (1999) *Science* **283,** 70–74.
18. Ikonomidou, C., Bittigau, P., Ishimaru, M. J., Wozniak, D. F., Koch, C., Genz, K., Price, M. T., Stefovska, V., Hörster, F., Tenkova, T., *et al.* (2000) *Science* **287,** 1056–1060.
19. DeOlmos, J. S. & Ingram, W. R. (1971) *Brain Res.* **33,** 523–529.
20. Gundersen, H. J. G., Bendtsen, T. F., Korbo, L. & West, M. J. (1988) *APMIS* **96,** 379–394.
21. Ishimaru, M. J., Ikonomidou, C., Tenkova, T. I., Der, T. C., Dikranian, K., Sesma, M. A. & Olney, J. W. (1999) *J. Comp. Neurol.* **408,** 461–476.
22. Ohmori, H., Ogura, H., Yasuda, M., Nakamura, S., Hatta, T., Kawano, K., Michikawa, T., Yamashita, K. & Mikoshiba, K. (1999) *J. Neurochem.* **72,** 1497–1506.
23. Huang, E. J. & Reichardt, L. (2001) *Annu. Rev. Neurosci.* **24,** 677–736.
24. Behl, C. & Manthey, D. (2000) *J. Neurocytol.* **29,** 351–359.
25. Hee Han, B. & Holtzman, D. M. (2000) *J. Neurosci.* **20,** 5775–5781.
26. Wlaz, P., Rolinski, Z., Kleinrok, Z. & Czuczwar, S. J. (1992) *J. Neural Transm. Gen. Sect.* **89,** 41–48.
27. Rataud, J., Debarnot, F., Mary, V., Pratt, J. & Stutzmann, J. M. (1994) *Neurosci. Lett.* **172,** 19–23.
28. Turski, W. A., Cavalheiro, E. A., Coimbra, C., da Penha Berzaghi, M., Ikonomidou-Turski, C. & Turski, L. (1987) *Brain Res.* **434,** 281–305.
29. Renfray, G., Schlinger, H., Jakubow, J. & Poling, A. (1989) *J. Pharmacol. Exp. Ther.* **248,** 967–973.
30. Walton, N. Y. & Treiman, D. M. (1989) *Epilepsy Res.* **4,** 216–221.
31. DeSarro, G., Di Paola, E. D., Aguglia, U. & De Sarro, A. (1996) *Pharmacol. Biochem. Behav.* **55,** 39–48.
32. Walker, M. C. (1998) *Curr. Opin. Neurol.* **11,** 149–154.
33. Kriel, R. L., Birnbaum, A. K. & Cloyd, J. C. (1999) in *Pediatric Neurology Principles and Practice*, eds. Swaiman, K. S. & Ashwal, S. (Mosby, St. Louis), pp. 692–718.
34. Walton, N. Y. & Treiman, D. M. (1992) *Epilepsy Res.* **12,** 199–205.
35. Dalby, N. O. & Nielsen, E. B. (1997) *Epilepsy Res.* **28,** 63–72.
36. Hengartner, M. O. (2000) *Nature* **407,** 770–776.
37. Venters, H. D., Dantzer, R. & Kelley, K. W. (2000) *Trends Neurosci.* **23,** 175–180.
38. Dobbing, J. & Sands, J. (1979) *Early Hum. Dev.* **3,** 79–83.
39. Trotter, A. & Pohlandt, F. (2000) *Ann. Med.* **32,** 608–614.